

ESR study of the Eu^{2+} g -value in the metallic phase of cubic hexaboride $\text{Ca}_{1-x}\text{Eu}_x\text{B}_6$ ($0.15 \leq x \leq 1.00$)

R. R. Urbano,¹ P. G. Pagliuso,¹ C. Rettori,¹ A. Malachias,² E. Granado,^{1,2} P. Schlottmann,³ Z. Fisk,⁴ and S. B. Oseroff⁵

¹Instituto de Física “Gleb Wataghin,” UNICAMP, 13083-970, Campinas-SP, Brazil

²Laboratório Nacional de Luz Síncrotron, C.P. 6192, 13084-971, Campinas-SP, Brazil

³Department of Physics and National High Magnetic Field Laboratory, Florida State University, Tallahassee, Florida 32306, USA

⁴Department of Physics, University of California at Davis, Davis, California 95616, USA

⁵San Diego State University, San Diego, California 92182, USA

(Received 14 October 2005; revised manuscript received 29 December 2005; published 29 March 2006)

The angular, magnetic field, and temperature dependence of the $\text{Eu}^{2+}(4f^7, S=7/2)$ g -value in $\text{Ca}_{1-x}\text{Eu}_x\text{B}_6$ ($0.15 \leq x \leq 1.00$) is measured by means of electron spin resonance at two microwave frequencies, 9.4 and 34.4 GHz. The g -value is found to be anisotropic and magnetic-field-dependent. The reduction with field of the positive g -shift is interpreted in terms of the exchange interaction between the localized $\text{Eu}^{2+}4f^7$ electrons with the conduction $\text{Eu}^{2+}5d$ -like electrons and B $2p$ -like holes. The angular, temperature, and x dependence of the anisotropy of the g -value can be attributed to demagnetization effects due to the platelet-like shape of the samples. High-resolution synchrotron x-ray diffraction experiments show the absence of distortions larger than $\delta a/a \sim 10^{-4}$. However, a mechanism for the anisotropy based on a weak tetragonal lattice distortion arising from the crystal surface cannot be excluded.

DOI: [10.1103/PhysRevB.73.115123](https://doi.org/10.1103/PhysRevB.73.115123)

PACS number(s): 71.10.Ca, 76.30.-v, 75.20.Hr, 75.50.Pp

I. INTRODUCTION

Over the past decades, the cubic hexaboride compounds RB_6 (R =rare/alkaline earths, space group 221, $Pm\bar{3}m$) have been the subject of intensive studies, both experimental and theoretical, due to their variety of exotic effects and interesting physical properties such as ferromagnetism, weak ferromagnetism, metal-insulator transition, large negative magnetoresistance, quadrupolar ordering, Jahn-Teller effect, superconductivity, heavy fermion, fluctuating-valence, and Kondo lattice behaviors.^{1–13} Among them, EuB_6 is particularly interesting because of the formation of magnetic polarons, changing the magnetic and transport properties, and the two transitions observed at $T_{c1}=15.3$ and $T_{c2}=12.7$ K.^{4,6,14} The one at T_{c1} is believed to correspond to the percolation transition of the polarons and is accompanied by a semimetal to metal transition, while below T_{c2} all Eu^{2+} spins participate in the ferromagnetic (FM) long-range order.

In previous reports,^{15,16} we have studied the evolution from insulator ($x=0$) to semimetal ($x=1.00$) in $\text{Ca}_{1-x}\text{Eu}_x\text{B}_6$ by measuring the $\text{Eu}^{2+}(4f^7, S=7/2)$ electron spin resonance (ESR) linewidth (ΔH). Due to the broken translational invariance, in an alloy each Eu^{2+} ion introduces a bound state in the gap of the insulator CaB_6 . Our results indicate that at $x \approx 0.15$, the bound states percolate leading to a metallic environment with a spin-flip relaxation process involving magnetic polarons and the symmetries of the Fermi surface. $x \approx 0.15$ corresponds to a site percolation of random nearest and next-to-nearest neighbor bonds. Note that the next-to-next-to-nearest neighbor bonds ([111] direction) are blocked by the large B_6 anions for the propagation of the electron wave functions.

In the present work, we report on the field dependence of the $\text{Eu}^{2+}(4f^7, S=7/2)$ ESR g -shift and its angular dependence. We explain the field dependence of the g -shift in

terms of the exchange interaction between the localized $\text{Eu}^{2+}4f^7$ electrons with the conduction $\text{Eu}^{2+}5d$ -like electrons and $\text{B}_6^{2-}2p$ -like holes. The angular dependence of the g -value and its T dependence can be attributed to demagnetizing effects associated to the platelet shape of the crystals. High-resolution synchrotron x-ray diffraction rules out the presence of a significant lattice distortion. However, an anisotropy of g based on a tetragonal lattice distortion below the x-ray resolution arising from the crystal surface cannot be ruled out.

II. EXPERIMENTAL

Single crystals of $\text{Ca}_{1-x}\text{Eu}_x\text{B}_6$ ($0.003 \leq x \leq 1.00$) were grown as described in Ref. 2. The structure and phase purity were checked by x-ray powder diffraction and the crystal orientation determined by Laue x-ray diffraction. The faces of natural growth of the crystals are called (001) planes. Most of the ESR experiments were done in platelet-like ($\sim 1.2 \times 0.9 \times 0.2$ mm³) single crystals, except for one crystal with a nearly cubic shape ($\sim 1.0 \times 0.8 \times 0.7$ mm³). The latter is used to investigate the origin of the g -value anisotropy. The ESR experiments were performed in a Bruker spectrometer using an X-band (9.48 GHz) TE₁₀₂ room- T cavity and a Q-band (34.48 GHz) cool split-ring cavity, both coupled to a T -controller using a helium gas flux system for $4.2 \leq T \leq 300$ K. The ESR spectra were analyzed in terms of Dyson's theory for the resonance line shape.¹⁷ In the pertinent range of T , the resistivity of our crystals changes from ~ 0.2 to ~ 1 m Ω cm, which corresponds to microwave (X and Q bands) penetration skin depths of about 5–10 μm . $M(T, H)$ measurements for $2 \leq T \leq 300$ K were taken in a Quantum Design SQUID-RSO dc-magnetometer. The Eu^{2+} concentration in our crystals was determined from Curie-

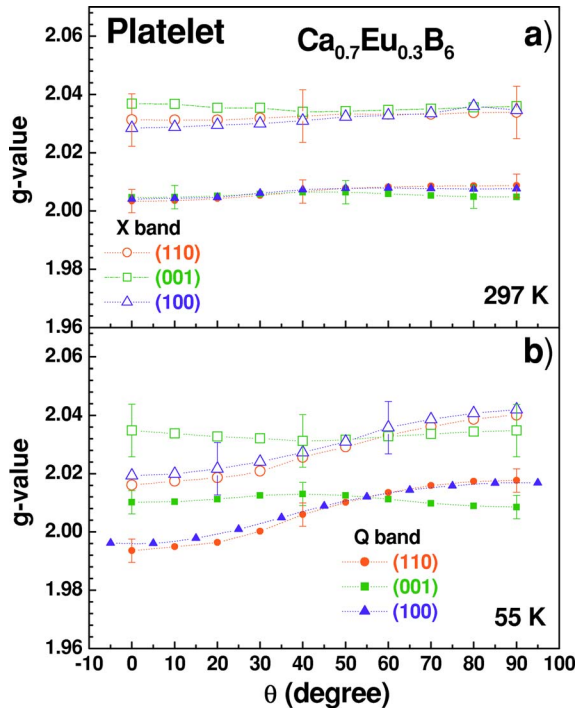


FIG. 1. (Color online) Angular dependence of the X- and Q-band ESR g -value for Eu^{2+} in a $\text{Ca}_{1-x}\text{Eu}_x\text{B}_6$ platelet-like single crystal for $x=0.30$ at room temperature and 55 K. The magnetic field H was rotated in the (001), (110), and (100) planes. $\theta=0$ corresponds to $H\parallel[001]$ in the planes (110) and (100) and to $H\parallel[100]$ in the plane (001).

Weiss fits of the susceptibility data. The ESR data presented in this work were obtained on the same samples used in our previous work.^{15,16} The high quality of the crystals is guaranteed by magnetoresistance and heat capacity measurements.^{15,16}

High-resolution synchrotron x-ray diffraction measurements were performed on the XRD-2 beamline¹⁸ at Laboratório Nacional de Luz Síncrotron (LNLS), Campinas, Brazil. An x-ray energy of 11999 eV was selected by a double-bounce Si(111) monochromator with water-refrigeration in the first crystal. In order to optimize angular and energy resolution, the beam was vertically collimated by a bent Rh-coated mirror placed before the monochromator. The energy resolution for this setup was 2.5 eV full width at half maximum. The sample was mounted on the cold finger of a commercial closed-cycle He cryostat ($10 \leq T \leq 300$ K) with a cylindrical Be window, which was fixed onto the Eulerian cradle of a commercial 4+2 circle diffractometer. The true 2θ diffraction angle of selected Bragg reflections was measured by a scintillation detector placed after a Ge(111) analyzer crystal.

III. RESULTS AND DISCUSSION

Figures 1 and 2 present the angular dependence of the g -value for the platelet-like crystals measured at X and Q bands in the (110), (100), and (001) planes at ~ 297 and ~ 55 K for $x=0.30$ and 1.00, respectively. Similar results

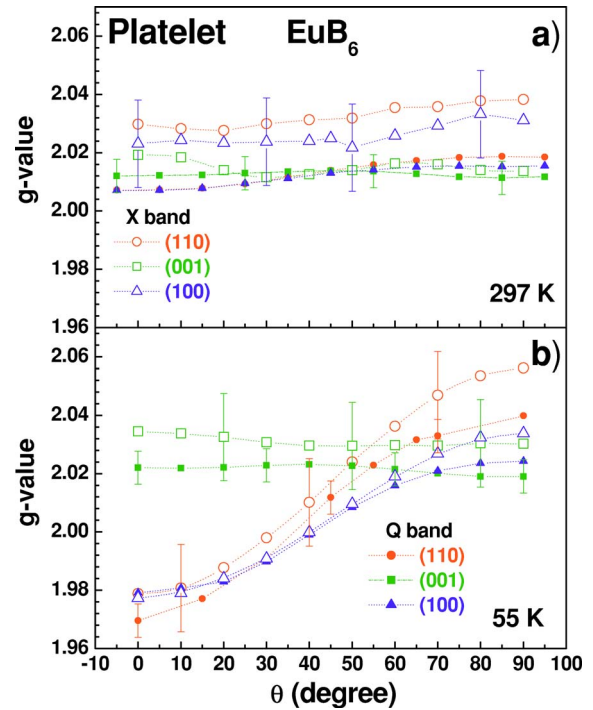


FIG. 2. (Color online) Angular dependence of the X- and Q-band ESR g -value for Eu^{2+} in an EuB_6 platelet-like single crystal at room temperature and 55 K. The magnetic field H was rotated in the (001), (110), and (100) planes. $\theta=0$ corresponds to $H\parallel[001]$ in the planes (110) and (100) and to $H\parallel[100]$ in the plane (001).

were obtained for the $x=0.60$ crystal (not shown here). The (001) plane coincides with the largest crystal face. The data show the following features: (i) The angular dependence of the g -value displays a tetragonal symmetry with the twofold axis being perpendicular to the largest crystal face,¹⁹ in spite of the overall cubic symmetry found for the anisotropy of the linewidth (see Figs. 6 and 7 in Ref. 16), (ii) the amplitude of the g -value anisotropy, $g_{\perp}-g_{\parallel}$, is nearly H - and x -independent, (iii) this amplitude increases at low- T , and (iv) the g -value decreases with H .

For the platelet-like crystals, Fig. 3(a) presents the room- T X- and Q-band ESR g -values for $\text{Ca}_{1-x}\text{Eu}_x\text{B}_6$ measured at the angle of minimum linewidth, i.e., along [111] for $x \geq 0.15$ and 30° from [001] in the (110) plane for $x \leq 0.10$ (see Ref. 16). Notice the increase of the g -value (positive g -shift) with increasing x at the percolation threshold of the impurity bound states ($x \approx 0.15$),¹⁶ and the reduction of the g -value at higher field (Q-band) as compared to the lower field (X-band) for $x \geq 0.15$. Figure 3(b) shows the g -shift ($\delta g = g - 1.988$) and Fig. 3(c) displays the amplitude of the g -value angular variation ($g_{\perp} - g_{\parallel}$). Within the experimental accuracy, the g -value, δg , and $g_{\perp} - g_{\parallel}$, are weakly x -dependent for $x \geq 0.15$, i.e., the metallic phase above the percolation threshold of the bound states.¹⁶ We should mention that for $x \leq 0.10$, i.e., for an insulating local environment of the Eu^{2+} ions, the g -value is isotropic within the experimental accuracy, but H -dependent (see Refs. 15, 16, and 20). The g -shift anisotropy is then to be associated with the metallic local environment (Dysonian line shape).

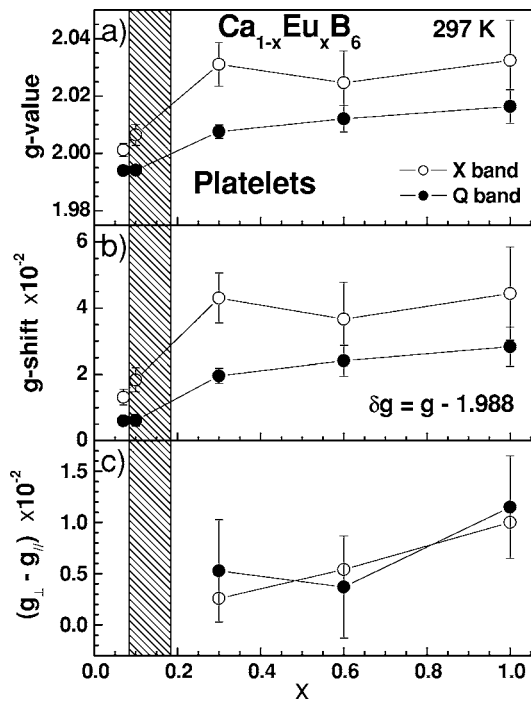


FIG. 3. (a) Room-temperature X- and Q-band g -values for platelet-like $\text{Ca}_{1-x}\text{Eu}_x\text{B}_6$ crystals measured at the angle of minimum linewidth (see text); (b) g -shift ($\delta g = g - 1.988$) corresponding to the data of (a); (c) amplitude of the g -value angular dependence ($g_{\perp} - g_{\parallel}$). g_{\perp} and g_{\parallel} correspond to the g -values for H_{\perp} and H_{\parallel} to $[001]$, respectively.

The reduction in the positive g -shift at high fields (see Q-band data in Figs. 1 and 2) may be understood in terms of a two-band model²¹ involving the exchange interaction between the localized $\text{Eu}^{2+}4f^7$ -electrons with (i) the conduction $\text{Eu}^{2+}5d$ -like electrons and (ii) the B $2p$ -like holes.²² The exchange interaction with the $5d$ -like electrons is assumed to be of atomic type, $J_{\text{at}}^e > 0$, and that with the B $2p$ -like holes of covalent origin, $J_{\text{cv}}^h < 0$. The magnitudes of the exchange constants have been estimated in Ref. 22 to be $|J_{\text{at}}^e| \approx 100$ meV and $|J_{\text{cv}}^h| \approx 5$ meV. The latter is expected to be small because of the almost ionic bond nature of the crystal, which locates the electrons close to the Eu^{2+} and the holes farther away in the neighborhood of the B_6^{2-} . Thus, the g -shift can be written as $\delta g = \delta g_e + \delta g_h = [J_{\text{at}}^e(0)\langle s_z^e \rangle + J_{\text{cv}}^h(0)\langle s_z^h \rangle]/(\mu_B H)$, where $J_{\text{at}}^e(0)$ and $J_{\text{cv}}^h(0)$ are the $q=0$ components (zero-momentum transfer between electrons),²³ and $\langle s_z^e \rangle$ and $\langle s_z^h \rangle$ are the spin-polarizations of the electrons and holes, respectively. The semimetal is not compensated, since it contains more electrons in the conduction band than holes in the valence band (B_6 deficiency). Since $|J_{\text{at}}^e| \gg |J_{\text{cv}}^h|$, the g -shift is dominated by the electrons and necessarily positive. For low fields the g -shift is then given by $\delta g = J_{\text{at}}^e(0)\eta_F^e + J_{\text{cv}}^h(0)\eta_F^h \approx J_{\text{at}}^e(0)\eta_F^e$, where η_F^e and η_F^h are the carrier densities of electrons and holes at the Fermi level, respectively. As the field increases, the atomic-like $5d$ -electrons spin-polarize and $\delta g \approx J_{\text{at}}^e(0)\langle s_z^e \rangle/(\mu_B H)$ decreases with H , as observed in Figs. 3(a) and 3(b). Note that

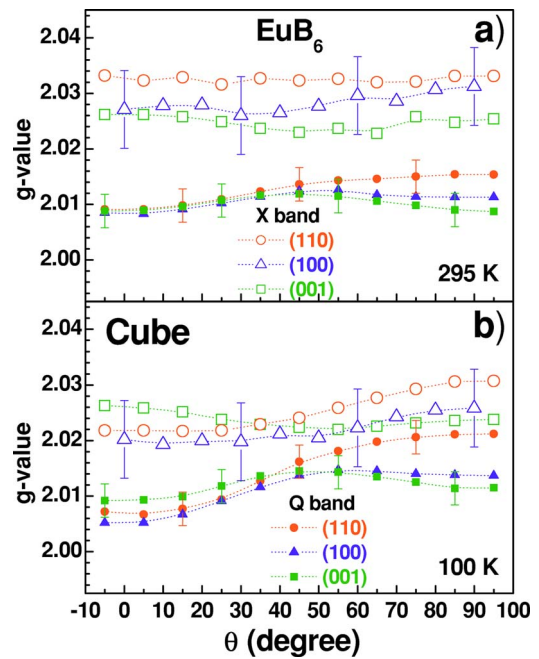


FIG. 4. (Color online) Angular dependence of the X- and Q-band ESR g -value for Eu^{2+} in an EuB_6 cube-shape single crystal at room temperature and 100 K. The magnetic field H was rotated in the (001), (110), and (100) planes. $\theta=0$ corresponds to $H_{\parallel}[001]$ in the planes (110) and (100) and to $H_{\parallel}[100]$ in the plane (001).

actually only the $5d$ -electrons are needed to explain the g -shift.

Within the accuracy of our experiments, the unexpected tetragonal symmetry revealed by the angular dependence of the g -value, shown in Figs. 1 and 2 for $x \geq 0.15$, has an amplitude that for ($T \gg T_{c1}$) only slightly increases with x and is nearly H -independent. Hence, it cannot be attributed to magnetic exchange or magnetic short-range-order effects. Below, we provide two plausible explanations for this symmetry reduction: (i) A lattice distortion, which might take place over the whole sample volume or just in the near-surface region, and (ii) the existence of significant angular-dependent demagnetizing fields arising from the platelet-like shape of the crystal. We elaborate on these mechanisms below.

Since the ESR signal in platelet-like crystals mainly arises from the Eu^{2+} ions within the microwave skin depth of the two largest crystal faces, data were also taken in a EuB_6 crystal with a nearly cubic-shape ($\sim 1.0 \times 0.8 \times 0.7$ mm³), rather than platelet-shaped. The total area of the lateral faces of the nearly cubic sample is slightly larger than the sum of the two largest faces of the platelet-shaped crystals. The angular dependence of the g -value for this crystal is presented in Fig. 4. For the quasicubic crystal, the angular dependence of the linewidth shows the same anisotropy with overall cubic symmetry found for the platelet-like crystals (see Refs. 15 and 16). The data in Fig. 4 show that the twofold symmetry observed for the g -value in the (100) plane of the platelet-like crystal (see Fig. 2) now displays a tendency

TABLE I. Measured values of $a^* = d\sqrt{h^2 + k^2 + l^2}$ for different (h, k, l) Bragg reflections, at 10 and 300 K. The x-ray penetration depth (z) for each reflection is also given.

(h, k, l)	a^* (Å)		z (μm)
	10 K	300 K	
(0 0 3)	4.1809(2)	4.1841(3)	3.2
(0 0 4)	4.1811(2)	4.1842(2)	4.3
(0 0 5)	4.1813(2)	4.1844(2)	5.4
(3 0 5)	4.1809(2)	4.1844(2)	3.6
(3 0 4)	4.1808(2)	4.1840(2)	0.4
(4 0 5)	4.1811(2)	4.1844(2)	3.3
(0 3 3)	4.1810(2)	4.1841(2)	3.3
(0 4 3)	4.1809(2)	4.1842(2)	3.4
(0 3 2)	4.1808(2)	4.1841(2)	2.1
(0 4 2)	4.1808(2)	4.1841(2)	2.3

toward a fourfold symmetry. The results suggest that there are actually three orthogonal axes of twofold symmetry, along each of the [001] crystal directions. This is the consequence of the six faces contributing approximately equally to the resonance shift. Also, the amplitude of the g -value anisotropy in the (110) plane was found to be smaller. Thus, the twofold symmetry observed in the (100) planes of Figs. 1 and 2 appears to be just a consequence of the platelet-like shape of the crystals. This appears to dismiss the hypothesis of a cooperative bulk lattice distortion in the compound.

A. Possibility of a surface induced lattice distortion

In an attempt to detect any near-surface tetragonal distortion, high-resolution synchrotron x-ray diffraction measurements were performed for EuB_6 at 10 and 300 K. A parallelepiped-shaped crystal with dimensions $3.0 \times 1.5 \times 1.2 \text{ mm}^3$ was taken from the same batch as the quasi-cubic-shaped EuB_6 sample studied by ESR. Table I shows $a^* = d\sqrt{h^2 + k^2 + l^2}$ for a set of $(00l)$, $(h0l)$, and $(0kl)$ Bragg reflections measured with the incident beam reaching the surface with the largest area, where d is the interplanar distance obtained from each diffraction angle 2θ . The crystal orientation is defined such that the c -direction is the normal to the sample surface irradiated by the x rays. The $\sim 12 \text{ keV}$ x-ray penetration depth z is also given for each reflection, being calculated using the relation $z = [\mu/\sin(\gamma) + \mu/\sin(\beta)]^{-1}$, where μ is the absorption coefficient of the material²⁴ and γ and β are the angles of incidence and emergence, respectively, of the x-ray beam with respect to the sample surface. For a homogeneous cubic material, a^* is independent of h , k , l , and z , and defines the cubic lattice parameter a . Instead, for cubic samples with depth-dependent strain and/or noncubic materials, a^* is expected to show variations for different reflections. The data in Table I indicate that a^* does not show any systematic variation with either z or (h, k, l) , within the experimental errors ($\sim 2 \times 10^{-4} \text{ \AA}$), revealing a homogeneous and cubic crystal structure for EuB_6 . Since a^* is found to be z -independent, the a , b , and c lattice parameters could

be extracted using the reflections shown in Table I. We thus obtain $a = 4.1808(3) \text{ \AA}$, $b = 4.1807(4) \text{ \AA}$, and $c = 4.1811(2) \text{ \AA}$ ($T = 10 \text{ K}$), and $a = 4.1842(4) \text{ \AA}$, $b = 4.1840(4) \text{ \AA}$, and $c = 4.1842(2) \text{ \AA}$ ($T = 300 \text{ K}$). We emphasize that the x-ray and microwave penetration depths are comparable in this case, indicating that the clear tetragonal symmetry found for the g -value (see above) takes place in a nearly cubic and homogeneous crystalline environment, in which the tetragonal distortion of the unit cell is below $\delta a/a \sim 10^{-4}$.

Within the skin depth of the microwaves, the g -value anisotropy may be caused by a *distortion* of the lattice, too small to be observable by our x-ray diffraction experiment. There are numerous ESR uniaxial stresses studies on Gd^{3+} and Eu^{2+} impurities in cubic crystals. The most appropriate comparison with the present case is insulating hosts with ionic bonding, e.g., CaF_2 or CaO .²⁵ A tetragonal uniaxial stress deforms the crystal and induces angular-dependent line shifts in the ESR spectra via the spin-lattice coefficients. The shifts are proportional to the applied pressure. Uniaxial pressures of the order of 10^9 dyn/cm^2 are already close to the rupture limit for the crystal and lead to barely perceptible line shifts for the S-state impurities, Gd^{3+} and Eu^{2+} . This corresponds to a crystal deformation $\delta a/a$ in the range of 4×10^{-4} , where a is the lattice constant. The g -value anisotropy observed in $\text{Ca}_{1-x}\text{Eu}_x\text{B}_6$ is much larger and of the order of that found for Gd^{3+} in crystals with tetragonal symmetry.²⁶ Furthermore, should this tetragonal deformation be much larger than 10^{-4} , then it would be detectable via diffraction experiments, but this has not been observed (see above and Ref. 7). Hence, the g -value anisotropy of Eu^{2+} cannot be induced by a tetragonal deformation through the Eu^{2+} spin-lattice coefficients. The spin-lattice coefficients are too small because Eu^{2+} is an S-state ion.

To conclude our discussion on a lattice deformation as the origin for the anisotropy of the g -value observed via ESR, we will briefly speculate on a mechanism capable of enhancing the effect of a small distortion. The spin-exchange of the $4f$ electrons with the $5d$ conduction electrons can lead to a substantial anisotropy, because even a small tetragonal crystalline field significantly affects the $5d$ levels. The $5d$ electrons in cubic symmetry split into e_g and t_{2g} orbitals. In eightfold coordination, the e_g is the ground doublet and the energy separation ($10Dq$) to the t_{2g} is large, so that only the e_g doublet needs to be considered. The tetragonal distortion lifts the degeneracy of the e_g doublet. In the absence of spin-orbit coupling, this splitting has no effect on the Eu^{2+} g -value. However, the spin-orbit coupling of the $5d$ electron, which competes with the quenching of the $5d$ orbits, induces the tetragonal symmetry in the Eu^{2+} g -value via the exchange coupling J_{at}^e . At high T , EuB_6 has only few conduction electrons and the number of electrons increases at low T . We then expect the anisotropy to be larger at low T . Furthermore, the magnetic field has no effect on the e_g doublet, so that the amplitude of the anisotropy should be independent of the field, and in the metallic phase of $\text{Ca}_{1-x}\text{Eu}_x\text{B}_6$ there should be no dramatic variation of the number of carriers with x at a given T , so that this effect should only depend weakly on x . The above trends are in agreement with the experimental findings.

The open question is the origin of the deformation. The binding energy of the crystal is predominantly ionic and given by the Madelung sum of the Coulomb interaction between all the ions. For the bulk, choosing an Eu^{2+} as the origin, this sum can be viewed as a sum over shells of equidistant (measured from the origin) ions. These shells have alternating charges, thus leading to effective (radial) dipolar contributions. Since the Coulomb interaction falls off only as the inverse of the distance, a very large number of shell pairs will contribute to the binding energy. At a distance z from the surface of the crystal, only spherical shells of radius less than z are complete. Shells of radius larger than z are incomplete in the direction of the surface and the dipoles contributing to the binding energy are missing. This imbalance introduces an axial symmetry and has as a consequence an elongation of the lattice spacing in the $[001]$ direction. For z of the order of the microwave penetration skin depth, the tetragonal distortion should be of the order of 10^{-4} of the lattice parameter. Hence, the crystal could have an effective tetragonal symmetry with $[001]$ being the fourfold axis.

B. Demagnetization effects

We now turn to investigate the possibility of demagnetizing effects causing the tetragonal symmetry of the g -value in the platelet-like samples. Although the ESR experiments were taken well above T_{c1} , due to the small dimensions of the crystals, the demagnetization factors may still be the origin of the observed g -value anisotropy.

As shown in Ref. 27, the resonance frequency in the presence of demagnetizing effects is given by

$$\omega_0^2 = \gamma^2 [H + (N_y - N_z)M][H + (N_x - N_z)M], \quad (1)$$

where N_x , N_y , and N_z are the components of the demagnetization tensor, $\gamma = e/mc$ is the gyromagnetic ratio for spins, and H and M are the magnetic field and the magnetization, both pointing in the z direction. For a paramagnet, $M = \chi H$, expression (1) reduces to

$$\omega_0^2 = \gamma^2 [1 + (N_y - N_z)\chi][1 + (N_x - N_z)\chi]H^2, \quad (2)$$

i.e., the resonance frequency is proportional to the field and hence the g -value is field independent.

The amplitude of the anisotropy is given by the difference between the g -values for H perpendicular and parallel to the plane of the platelet. Assuming an infinite thin plane and the field perpendicular to the plane, we have $N_x = N_y = 0$ and $N_z = 4\pi$, so that $\omega_0^{\parallel} = \gamma(1 - 4\pi\chi)H$. On the other hand, for the field in the plane of the platelet, we have $N_y = 4\pi$ and $N_x = N_z = 0$, so that $\omega_0^{\perp} = \gamma(1 + 4\pi\chi)^{1/2}H$. Assuming that $4\pi\chi$ is small compared to 1, the amplitude of the anisotropy is then approximately $\delta\omega_0/H = \gamma 6\pi\chi$. The temperature dependence of the anisotropy arises from the magnetic susceptibility, χ , which increases as the temperature is lowered.

The susceptibility has been studied in detail in Ref. 6. It displays a Curie-Weiss-like behavior consistent with the magnetic moment of Eu^{2+} and the ferromagnetic ordering temperature T_{c2} . The high-temperature Curie constant (and the effective magnetic moment) depends slightly on the direction of the field with respect to the crystal axis. This de-

pendence could arise from a small orbital contribution induced from excited states of Eu^{2+} via spin-orbit interaction and is consistent with the fine-structure observed in the ESR spectra. It does not necessarily imply a presence of demagnetization effects.

We now insert an average value of the susceptibility from Fig. 6 of Ref. 6 into the amplitude of the anisotropy for room temperature and 55 K, to compare with the experimental values shown in Fig. 2. We choose $\chi_{\text{mol}} = 0.029$ emu/mole at 297 K and $\chi_{\text{mol}} = 0.20$ emu/mole for 55 K. Using the mass density (4.92 g/cm³) and the molar mass (217 g/mol) for EuB_6 , the molar susceptibility is transformed into the magnetic susceptibility, i.e., $\chi = 0.00066$ at 297 K and $\chi = 0.00453$ at 55 K. This leads to an anisotropy of g , i.e., $g_{\perp} - g_{\parallel} = 12\pi\chi$, of 0.025 at room temperature and 0.171 at 55 K.

These calculated values are considerably larger than the observed ones, i.e., by a factor 2.5 and 4, respectively. A possible reason for the overestimate is that the platelets are not infinitesimally thin and infinite in the x and y direction. More realistic values for the components of the demagnetization tensor tend to reduce the amplitude of the anisotropy. The results also reproduce the magnetic field independence of the anisotropy of g . The x dependence of the anisotropy has a large experimental uncertainty, but the correct trends can be explained as well. Assuming that the paramagnetic susceptibility is proportional to x , then also $g_{\perp} - g_{\parallel}$ is proportional to x . The experimental findings indicate that this is roughly the case.

IV. CONCLUSIONS

In summary, we have reported the field and angular dependence of the g -value in the ESR of $\text{Ca}_{1-x}\text{Eu}_x\text{B}_6$ for $0.30 \leq x \leq 1.00$. It was found that the g -shift is reduced with the field. This is explained in terms of an exchange interaction between the localized $\text{Eu}^{2+}4f^7$ -electrons with $5d$ -like electrons, which are rapidly polarized by the magnetic field, since $\text{Ca}_{1-x}\text{Eu}_x\text{B}_6$ is a low carrier density system. The B_{2p} -like holes do not play a major role in this context.

Two mechanisms for the surprising tetragonal angular dependence of the g -value found even at temperatures well above $T_{c1} \approx 15$ K have been proposed. (i) A tetragonal crystal distortion of the lattice within or beyond the microwave skin depth could induce such g -anisotropy. High-resolution synchrotron x-ray diffraction measurements exclude the possibility of distortions larger than $\delta a/a \sim 10^{-4}$. This, however, does not eliminate a distortion-based anisotropy, but makes this venue less plausible. (ii) The existence of significant angular-dependent demagnetizing fields arising from the platelet-like shape of the crystal can give rise to such an anisotropy. Although quantitative estimates are difficult, an idealized thin plane of infinite dimensions yields values for $g_{\perp} - g_{\parallel}$ that are compatible in magnitude and in trends as a function of x , H , and T with the experiments.

ACKNOWLEDGMENTS

The work at UNICAMP and LNLS is supported by FAPESP, CNPq, and ABTLuS, and the work at the NHMFL

by NSF Cooperative Agreement No. DMR-9527035 and the State of Florida. The support by NSF (Grants No. DMR-

0102235 and No. DMR-0105431) and DOE (Grant No. DE-FG02-98ER45797) is also acknowledged.

-
- ¹J. Etourneau and P. Hagenmuller, *Philos. Mag. B* **52**, 589 (1985).
- ²D. P. Young, D. Hall, M. E. Torelli, Z. Fisk, J. L. Sarrao, J. D. Thompson, H. R. Ott, S. B. Oseroff, R. G. Goodrich, and R. Zysler, *Nature (London)* **397**, 412 (1999).
- ³M. E. Zhitomirsky, T. M. Rice, and V. I. Anisimov, *Nature (London)* **402**, 251 (1999).
- ⁴L. Degiorgi, E. Felder, H. R. Ott, J. L. Sarrao, and Z. Fisk, *Phys. Rev. Lett.* **79**, 5134 (1997).
- ⁵S. Massidda, A. Continenza, T. M. de Pascale, and R. Monnier, *Z. Phys. B: Condens. Matter* **102**, 83 (1997).
- ⁶S. Süllow, I. Prasad, M. C. Aronson, J. L. Sarrao, Z. Fisk, D. Hristova, A. H. Lacerda, M. F. Hundley, A. Vigliante, and D. Gibbs, *Phys. Rev. B* **57**, 5860 (1998).
- ⁷C. H. Booth, J. L. Sarrao, M. F. Hundley, A. L. Cornelius, G. H. Kwei, A. Bianchi, Z. Fisk, and J. M. Lawrence, *Phys. Rev. B* **63**, 224302 (2001).
- ⁸S. Paschen, D. Pushin, M. Schlatter, P. Vonlanthen, H. R. Ott, D. P. Young, and Z. Fisk, *Phys. Rev. B* **61**, 4174 (2000).
- ⁹G. A. Wigger, Ch. Walti, H. R. Ott, A. D. Bianchi, and Z. Fisk, *Phys. Rev. B* **66**, 212410 (2002).
- ¹⁰G. A. Wigger, C. Beeli, E. Felder, H. R. Ott, A. D. Bianchi, and Z. Fisk, *Phys. Rev. Lett.* **93**, 147203 (2004).
- ¹¹G. Uimin, *Phys. Rev. B* **55**, 8267 (1997).
- ¹²H. Sturm, B. Elschner, and K.-H. Hock, *Phys. Rev. Lett.* **54**, 1291 (1985).
- ¹³T. S. Al'tshuler and M. S. Bresler, *JETP* **88**, 1019 (1999) T. S. Al'tshuler and M. S. Bresler, [*JETP* **115**, 1860 (1999)].
- ¹⁴S. Süllow, I. Prasad, M. C. Aronson, S. Bogdanovich, J. L. Sarrao, and Z. Fisk, *Phys. Rev. B* **62**, 11626 (2000).
- ¹⁵R. R. Urbano, P. G. Pagliuso, C. Rettori, S. B. Oseroff, J. L. Sarrao, P. Schlottmann, and Z. Fisk, *Phys. Rev. B* **70**, 140401(R) (2004).
- ¹⁶R. R. Urbano, P. G. Pagliuso, C. Rettori, P. Schlottmann, J. L. Sarrao, A. Bianchi, S. Nakatsuji, Z. Fisk, E. Velazquez, and S. B. Oseroff, *Phys. Rev. B* **71**, 184422 (2005).
- ¹⁷G. Feher and A. F. Kip, *Phys. Rev.* **98**, 337 (1955); F. J. Dyson, *Phys. Rev.* **98**, 349 (1955); G. E. Pake and E. M. Purcell, *ibid.* **74**, 1184 (1948).
- ¹⁸C. Giles, F. Yokaichiya, S. W. Kycia, L. C. Sampaio, D. C. Ardiles-Saravia, M. K. K. Franco, and R. T. Neuenschwander, *J. Synchrotron Radiat.* **10**, 430 (2003).
- ¹⁹A. Abragam and B. Bleaney, *EPR of Transition Ions* (Clarendon Press, Oxford, 1970).
- ²⁰S. Kunii, T. Uemura, Y. Chiba, T. Kasuya, and M. Date, *J. Magn. Magn. Mater.* **52**, 271 (1985); S. Kunii, *J. Phys. Soc. Jpn.* **69**, 3789 (2000).
- ²¹P. M. Bisch, A. Troper, and A. A. Gomes, *Phys. Rev. B* **13**, 3902 (1976); A. Troper, O. L. T. de Menezes, P. Lederer, and A. A. Gomes, *ibid.* **18**, 3709 (1978); G. E. Barberis, D. Davidov, J. P. Donoso, C. Rettori, J. F. Suassuna, and H. D. Dokter, *ibid.* **19**, 5495 (1979); P. G. Pagliuso, C. Rettori, J. L. Sarrao, A. Cornelius, M. F. Hundley, Z. Fisk, and S. B. Oseroff, *ibid.* **60**, 13515 (1999).
- ²²M. J. Calderón, L. G. L. Wegener, and P. B. Littlewood, *Phys. Rev. B* **70**, 092404 (2004).
- ²³D. Davidov, K. Maki, R. Orbach, C. Rettori, and E. P. Chock, *Solid State Commun.* **12**, 621 (1973).
- ²⁴B. L. Henke, E. M. Gullikson, and J. C. Davis, *At. Data Nucl. Data Tables* **54**, 181 (1993); see also www-cxro.lbl.gov.
- ²⁵R. Calvo, R. A. Isaacson, and Z. Sroubek, *Phys. Rev.* **177**, 484 (1969); S. Oseroff and R. Calvo, *Phys. Lett.* **32A**, 393 (1970).
- ²⁶C. Rettori, D. Rao, S. Oseroff, R. D. Zysler, M. Tovar, Z. Fisk, S.-W. Cheong, S. Schultz, and D. C. Vier, *Phys. Rev. B* **44**, 826 (1991).
- ²⁷Ch. Kittel, *Phys. Rev.* **73**, 155 (1948).